

Article

Compression Ignition Internal Combustion Engine's Energy Parameter Research Using Variable (HVO) Biodiesel and Biobutanol Fuel Blends

Gintaras Valeika¹, Jonas Matijošius^{2,*}, Olga Orynych^{3,*}, Alfredas Rimkus¹, Artūras Kilikevičius² and Karol Tucki^{4,*}

¹ Department of Automobile Engineering, Faculty of Transport Engineering, Vilnius Gediminas Technical University, J. Basanavičiaus Str. 28, LT-03224 Vilnius, Lithuania; gintaras.valeika@vilniustech.lt (G.V.); alfredas.rimkus@vilniustech.lt (A.R.)

² Mechanic Science Institute, Vilnius Gediminas Technical University, Plytinės Str. 25, LT-10105 Vilnius, Lithuania; arturas.kilikevicius@vilniustech.lt

³ Department of Production Management, Faculty of Engineering Management, Bialystok University of Technology, Wiejska Street 45A, 15-351 Bialystok, Poland

⁴ Department of Production Engineering, Institute of Mechanical Engineering, Warsaw University of Life Sciences, Nowoursynowska Street 164, 02-787 Warsaw, Poland

* Correspondence: jonas.matijosius@vilniustech.lt (J.M.); o.orynych@pb.edu.pl (O.O.); karol_tucki@sbgw.edu.pl (K.T.); Tel.: +48-746-98-40 (O.O.); +48-593-45-78 (K.T.)

Abstract: This study investigates the impact of different biofuels, such as pure hydrogenated vegetable oil, hydrogenated vegetable oil, and biobutanol, as well as their blends, on the non-energetic operational characteristics of a compression ignition internal combustion engine. The research investigations were conducted using a turbocharged direct injection compression ignition engine that was put within a Skoda Octavia 1.9 TDI automobile. Throughout the investigation, the primary emphasis was placed on analyzing energy characteristics such as power, brake-specific fuel consumption (BSFC), brake thermal efficiency (BTE), and other related factors. The analysis involved the utilization of multiple combinations of bio-based fuels, namely four mixes of HVO with biobutanol (HVO100, HVOB5, HVOB10, and HVOB20), which were subsequently compared to fossil diesel (D100). The findings of the study indicate that the utilization of HVO100 fuel results in notable reductions in power output and mass fraction when compared to D100 gasoline. HVO100 fuel demonstrates superior performance to D100 gasoline, exhibiting a range of 1.7% to 28% improvement in brake-specific fuel consumption. Additionally, at an engine speed of 4500 rpm, the use of HVO100 fuel leads to a decrease in brake thermal efficiency of 4.4%.

Keywords: vehicle; HVO and biobutanol fuel blends; biofuels; engine's power; BSFC; BTE



Citation: Valeika, G.; Matijošius, J.; Orynych, O.; Rimkus, A.; Kilikevičius, A.; Tucki, K. Compression Ignition Internal Combustion Engine's Energy Parameter Research Using Variable (HVO) Biodiesel and Biobutanol Fuel Blends. *Energies* **2024**, *17*, 262. <https://doi.org/10.3390/en17010262>

Academic Editor: Albert Ratner

Received: 9 October 2023

Revised: 7 November 2023

Accepted: 16 November 2023

Published: 4 January 2024



Copyright: © 2024 by the authors. Licensee MDPI, Basel, Switzerland. This article is an open access article distributed under the terms and conditions of the Creative Commons Attribution (CC BY) license (<https://creativecommons.org/licenses/by/4.0/>).

1. Introduction

The heightened consciousness throughout society regarding the detrimental effects of the road transport industry on the environment necessitates the implementation of more aggressive and transformative measures [1,2]. These activities primarily concentrate on the domains of legislation, technology, and fuel. The adverse effects of climate change and the persistent degradation of the environment present a significant risk to Europe and the global community as a whole [3,4].

Based on data provided by the European Environment Agency, it is seen that almost one-fourth of the European Union's aggregate carbon dioxide (CO₂) emissions in the year 2019 originated from the transportation sector. Notably, road transport accounted for 71.7% of these emissions [5]. The European Commission has recently implemented a comprehensive set of legislative propositions aimed at harmonizing the European Union's climate, energy, transport, and tax policies [6,7]. The primary objective of these recommendations is

to achieve a substantial reduction in net greenhouse gas emissions, targeting a minimum decrease of 55 percent by the year 2030 in comparison to the emission levels recorded in 1990. In accordance with the European Green Deal, there is a pressing need to curtail CO₂ emissions and attain climate neutrality by 2050 [8]. To this end, it is imperative to achieve a 90% reduction in greenhouse gas emissions by 2050, relative to the levels seen in 1990 [9,10].

The European Union has been implementing measures over an extended period of time in order to mitigate the adverse effects of human activities on the environment [11,12]. One example of such endeavors involves the implementation of a series of laws that establish acceptable thresholds for exhaust emissions produced by automobiles sold within the European market. These regulations, known as the Euro exhaust emission standards (EURO), serve as a framework for governing the permitted levels of emissions [13–15]. The primary objective is to mitigate the adverse effects of road transportation on the environment and public health through the regulation of air pollutants, including nitrogen oxides (NO_x), particulate matter (PM), hydrocarbons (HC), and carbon dioxide (CO₂) [16–18]. The Euro 6d-ISC-FCM standard has been implemented since 2021. From a technology standpoint, these standards mandate the installation of fuel consumption monitoring devices in passenger vehicles [19–21]. Drawing on the literature, a comparative analysis can be conducted to assess the disparity between the quantities of pollutants discharged into the atmosphere by a vehicle during real-world driving conditions and the emission values officially reported by the manufacturer. Presently, in order to avoid financial penalties, automotive corporations are required to uphold an average carbon dioxide emission level of 95 g/km across all vehicles manufactured. In 2019, the mean carbon dioxide (CO₂) emissions produced by automobiles registered within the European Union (EU) amounted to 122.4 g per kilometer. This figure exceeded the relevant regulatory threshold by an additional 27.4 g [22].

Standardized measuring testing is conducted on all newly manufactured automobiles [23,24]. The WLTP (Worldwide Harmonized Light Vehicles Test Procedure) driving cycle was implemented in September 2018, replacing the previously used New European Driving Cycle (NEDC) [25,26]. Furthermore, the Real Driving Emissions (RDE) emission test is employed to directly assess pollutant emissions while vehicles are in operation on public roads [27,28].

The European Union (EU) places significant emphasis on the promotion of issues pertaining to alternative fuels [29,30]. Biofuels derived from biomass for transportation purposes are regarded as a very promising category of alternative fuels with the potential to mitigate dependence on petroleum-based fuels and contribute to environmental sustainability [31,32].

The term “biofuel” encompasses a broad range of interpretations and encompasses a diverse array of substrates. Liquid or gaseous biofuels serve as a viable substitute for diesel oil due to their composition, which includes plant biocomponents such as rapeseed, soybean, sunflower, palm oil, and other oil plants. This composition contributes to a reduction in the use of petroleum-based fuels [33,34].

Biofuels can be categorized based on their physical state, the generation of production technique employed (first, second, or third generation), the type of engine they are used to power (compression ignition or spark ignition), or their specific application [35,36]. Biodiesel, classified as a first-generation biofuel, is widely recognized as the prevailing kind of biofuel. It mostly consists of methyl or ethyl esters of fatty acids, commonly referred to as Fatty Acid Methyl Esters (FAME) or Fatty Acid Ethylesters (FAEE) [37–40]. The primary methods employed in their manufacturing include esterification, transesterification, and cold pressing. Second-generation biofuels are derived only from waste biomass or substances that are not acceptable for use as food. Biohydrocarbons are a specific category of biocomponents that are added to biofuels as an admixture. The production of these substances involves the use of catalytic oil hydrogenation technology, a process that entails the elimination of oxygen and unsaturated bonds from triglyceride structures (known as hydrotreated vegetable oils—HVO) [41–43]. The resulting composition predominantly

consists of liquid paraffinic hydrocarbons. The primary source of third-generation biofuels is predominantly derived from algae [44,45].

The European Union has been actively advocating for the advancement of electromobility in recent years. Battery electric vehicles (BEVs) are characterized by their emission-free nature during operation. The ecological impact of these entities is contingent upon the energy source used for their operation. The use of renewable energy sources (RES) for charging purposes ensures that the indirect emissions associated with an electric vehicle are primarily confined to its production phase. The factors that contribute to a lack of faith in this particular technical solution encompass deficiencies in the technical infrastructure, concerns over fire safety, and potential electromagnetic interference [46,47].

Many experts hold the view that investments in technology pertaining to electromobility are of a transitory nature. The focal solution pertains to hydrogen technologies [48]. The expeditious establishment of a competitive hydrogen production sector is of utmost importance, as it serves as a safeguard against political instability and has the potential to enhance the competitiveness and trade balance of numerous nations. The use of hydrogen will hold significant significance for economic sectors that face challenges in achieving decarbonization through direct electrification. This encompasses various sectors, including but not limited to transportation (road, sea, and rail) and industrial operations that necessitate elevated temperatures, such as the production of steel. Support is necessary for the development of both electric vehicle charging and hydrogen refueling infrastructures [49,50].

Primary biofuels and processed biofuels are the two categories that can be used to classify biofuels [51,52]. Primary biofuels are fuels that are produced from natural, unprocessed biomass and that may be used directly to generate heat and energy [53,54]. An example of a primary biofuel is firewood. Fuels that have been processed are referred to as processed biofuels. These fuels can be generated by processing biomass using a variety of different processes. Biofuels that have been processed can be classified as either first-, second-, or third-generation biofuels. First-generation biofuels are largely oxygen compounds, such as ethyl alcohol, fatty acid methyl esters (FAME), and ethers. These first-generation biofuels are created using biomethanol and bioethanol as their starting materials. Higher fuel stability during fuel storage and distribution is one advantage that hydrocarbon biofuels and second-generation biocomponents have over first-generation biofuels. This advantage is gained by comparing first-generation biofuels to second-generation biocomponents [55]. The production of bioethanol from lignocellulosic raw materials is one example. Other examples include the production of synthetic fuels from syngas produced by the gasification of biomass and the production of hydrocarbon fuels through the hydroconversion process (for example, HVO) [56]. It is possible to manufacture second-generation biofuels based on waste biomass, such as that which contains organic components of municipal garbage, waste vegetable oils and animal fats, or pure vegetable oils acquired from crops grown in degraded areas that are unfit for use in the food business. Microalgae are the primary component of biofuels of the third generation.

First-generation biofuel conversion procedures involve cold pressing, extraction, and transesterification in order to produce biodiesel [57]. This biodiesel is comprised of rapeseed oil methyl esters (RME) or methyl esters (FAME) and ethyl esters (FAEE) of higher fatty acids derived from other oil plants. The majority of FAME comes from the transesterification of various vegetable oils. HVO is a type of fuel that can be produced using a process known as catalytic hydrogenation. During this process, oxygen and unsaturated bonds are eliminated from triglyceride structures. In contrast to fatty acid methyl esters, HVO does not precipitate paraffin even at temperatures 20 degrees below zero, which results in a reduction of 10%. Mineral fuels have a cetane number that ranges from 70 to 90, do not include sulfur or aromatic hydrocarbons, and have zero nitrogen oxide emissions; however, diesel fuel made from minerals only has a cetane value of 51. The standards for fuels do not specify a maximum level of HVO concentration; rather, they demand simply that the finished product, in the form of diesel oil, meets the quality requirements that are specified

in the standard. In actuality, diesel fuel can have between 20 and 30 percent HVO and an additional 7 percent FAME added to it.

Biofuels and alternative fuels for spark-ignition engines include ethanol, methanol, ethers, hydrocarbon synthetic fuels, liquefied petroleum gas, and hydrogen [58–60]. These fuels are also regarded as alternatives. In the field of powering compression-ignition engines, work is currently being carried out to obtain and use the following alternative fuels derived primarily from biomass: fatty acid esters (FAME and FAEE, from transesterification processes of rapeseed, sunflower, and soybean oils), dimethyl ether, fuel emulsions (water, pure vegetable oils, and hydrocarbon synthetic fuels), and fatty acid esters (FAME and FAEE). Fermentation and distillation are the two basic processes involved in the manufacturing of ethanol [61]. Using this method to produce fuel results in high overall production costs. Utilizing alternative substrates, such as waste cellulosic or lignocellulosic material, can help bring down the overall cost of production.

Diesel and natural gas are the two fuels that are used the most frequently to power generators; however, there are additional possibilities available. The performance of generator engines that are powered by renewable liquid fuels is comparable to the performance of generator engines that are driven by conventional diesel; however, there is a slight decrease in power as well as in fuel economy. The low-temperature characteristics of HVO and biodiesel must be suitable for the surroundings of the generator in order for them to be used.

When compared to the expenses of getting mineral fuels, the costs of manufacturing biofuels are significantly higher. The price of the raw material accounts for between 55 and 70 percent of the total production expenses; therefore, it has a significant impact on the overall cost of manufacturing biofuels. Due to this, many nations around the world encourage this industry by implementing administrative and fiscal restrictions on the biofuel market. This is carried out in the hopes of increasing the use of biofuels and, as a result, achieving the societal goals that have been presupposed. The availability and steadily increasing cost of the essential raw materials for production is the primary obstacle that all manufacturers of biocomponents are currently confronted with.

2. Materials and Methods

The vehicle used for the experiments was the Skoda Octavia, equipped with a 1.9-L TDI (Turbocharged Direct Injection) compression ignition engine, namely the type 1Z. This particular engine configuration consists of four cylinders and possesses a displacement of 1896 cm³. The engine exhibits a maximum power output of 66 kilowatts (kW) at an engine speed of 4000 revolutions per minute (rpm), while its maximum torque is recorded at 182 Newton meters (Nm) at an engine speed of 1900 rpm. Table 1 presents detailed information regarding the 1.9 TDI engine [62].

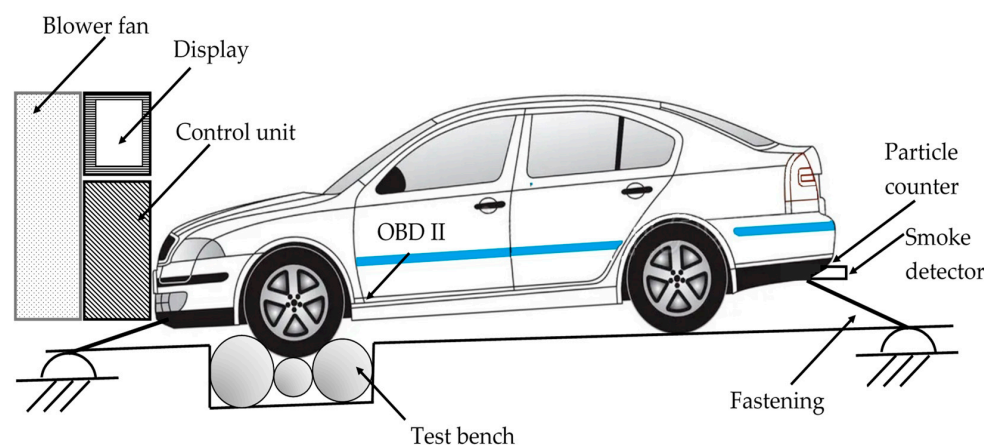
Table 1. The main parameters of the test engine (1.9 TDI type: 1Z) [62].

Parameter	Value
Engine type—number of cylinders	Inline 4
Engine code	ALH
Fuel type	Diesel
Engine alignment	Transverse
Engine displacement	1896 cm ³
Bore x Stroke	79.5 × 95.5 mm
Number of valves	8 Valves
Aspiration	Turbo
Maximum power	66 kW (4000 rpm)
Maximum torque	210 Nm (1900 rpm)
Drive wheels	FWD
Piston diameter, mm	79.5 mm
Piston stroke, mm	95.5 mm

Table 1. *Cont.*

Parameter	Value
Compression ratio	19.5
Displacement	1896 cm ³
Number of cylinders	4/OHC
Fuel injection	Direct (single)
Nozzle type	Hole-type
Nozzle opening pressure	190 bar
Nozzle and holder assembly	Two spring
Cooling system type	Liquid cooling
Transmission gearbox—number of speeds	5 speed Manual

The torque and power of the engine in a Skoda Octavia equipped with a 1.9-L TDI diesel engine, namely the type 1Z, were assessed using a computerized vehicle test bench known as the MAHA LPS 2000 (as depicted in Figure 1 and detailed in Table 2).

**Figure 1.** Laboratory testing apparatus.**Table 2.** The main parameters of the vehicle load bench (MAHA LPS 2000) [63].

Parameter	Value
Load equipment	Electromagnetic brake
Rate adjustment limits	260
Maximum measuring load	6 kN (attractive force)
Maximum break power, kW	260
Measurement error	±2%

During the experimental tests, the ROSS-TECH VCDS diagnostic tool was employed to retrieve data from the Electronic Control Unit (ECU) of the vehicle through an OBDII connection. The car diagnostic system known as ROSS-TECH VCDS collected data at regular intervals of 2.50 s [64–66].

The examination of engine ECU (electronic control unit) data revealed that the recorded data points, including engine speed (rpm), cyclic fuel quantity (mg/cycle), cyclic air mass (mg/cycle), fuel injection timing (°BTDC), turbocharger pressure (mbar), and fuel injection timing (mg/cycle), are transmitted in distinct blocks and lack precise synchronization in time.

Three sets of experiments were performed using the MAHA LPS 2000 vehicle test bench. During these studies, ECU data was recorded, and engine external speed parameters were measured.

The trials involved using an aggregate total of five distinct fuels and blends. The tested fuel samples encompassed several compositions, namely D100 (normal diesel), HVO100

(pure hydrotreated vegetable oil), 95/5, 90/10, and 80/20 (vol/vol) combinations of hydrotreated vegetable oil and biobutanol, as well as blends branded as HVOB5, HVOB10, and HVOB20. In order to enhance the lubricity of biobutanol blends, the inclusion of castor oil at a concentration of 5% by volume was implemented. The findings pertaining to the characteristics of pristine fuels are shown in Tables 3 and 4.

The effective use of biobutanol requires the incorporation of specialized fuel additives or a fuel component that provides lubrication, as biobutanol diminishes the lubricating properties of the fuel blend. The selection of castor oil as a lubricant is attributed to its cost-effectiveness and the avoidance of expensive compatibility tests associated with the use of specialized additives.

The physicochemical parameters of the fuel were verified by using literature data and fuel characteristics provided by the manufacturer [67,68].

Table 3. Properties of 100% pure diesel, hydrotreated vegetable oil, biobutanol, and castor oil [69–72].

Parameter	Diesel	HVO	Biobutanol	Castor Oil
Density at 15 °C, kg/m ³	835.2	779.1	810.0	964.4
Element composition: (% mass): Carbon	86.50	84.80	65.00	73.80
Hydrogen	13.40	15.30	13.55	11.50
Oxygen	0.0	0.0	21.50	14.85
Stoichiometric AFR	14.79	15.18	11.30	11.91
Cetane number	51	70	18	28
Lower heating value, MJ/kg	43.09	44.9	33.3	43.1
Lower heating value, MJ/L	36.90	34.10	26.71	39.81
Purity, %	N/A	N/A	99.5	100
Manufacturer, City, Country	Orlean Lietuva, Juodeikiai, Lithuania	Neste, Espoo, Finland	Carl Roth GmbH, Karlsruhe, Germany	Biochemlit, Kaunas, Lithuania

Table 4. Properties of fuel mixtures.

Properties	HVOB5	HVOB10	HVOB20
Density at 15 °C, kg/m ³	780.5	782.4	786.4
Element composition: (% mass): Carbon	83.45	82.55	80.58
Hydrogen	15.32	15.25	15.03
Oxygen	1.11	2.21	4.41
Stoichiometric AFR	14.99	14.77	14.38
Cetane number	67.3	64.7	59.3
Lower heating value, MJ/kg	43.55	42.98	41.88
Lower heating value, MJ/L	33.98	33.64	32.93

3. Results

Figure 2 depicts the relationship between engine load and fuel composition across various engine speeds. The conventional diesel engine is capable of achieving a maximum torque of 190 Nm. The use of HVO100 fuel resulted in a reduction of 10% in this metric when compared to the use of D100 gasoline. The gradual addition of biobutanol to HVO fuel, increasing from 5% to 20%, resulted in a consistent drop in torque, with reductions of 11%, 15%, and 18% seen at each respective increment. Figure 3 displays engine power characteristics, exhibiting a similar pattern. The use of D100 gasoline results in a maximum

power output of 64.5 kW, whereas HVO100 fuel exhibits a decrease in power output of 8%. Similarly, HVOB5 fuel demonstrates a reduction in power output of 11%, HVOB10 by 17%, and HVOB20 by 22% when compared to D100 fuel. The observed outcomes can be attributed to the reduced lower heating value (LHV) values, as indicated in Tables 4 and 5. While the lower heating value of hydrotreated vegetable oil (HVO100) is higher than that of conventional diesel in terms of MJ/kg, it is important to note that the density of HVO100 is significantly lower than that of conventional diesel. Consequently, the lower heating value of HVO100, expressed in MJ/L, is lower when compared to D100, HVOB5, HVOB10, and HVOB20. This decrease in value is observed consistently across these fuel types.

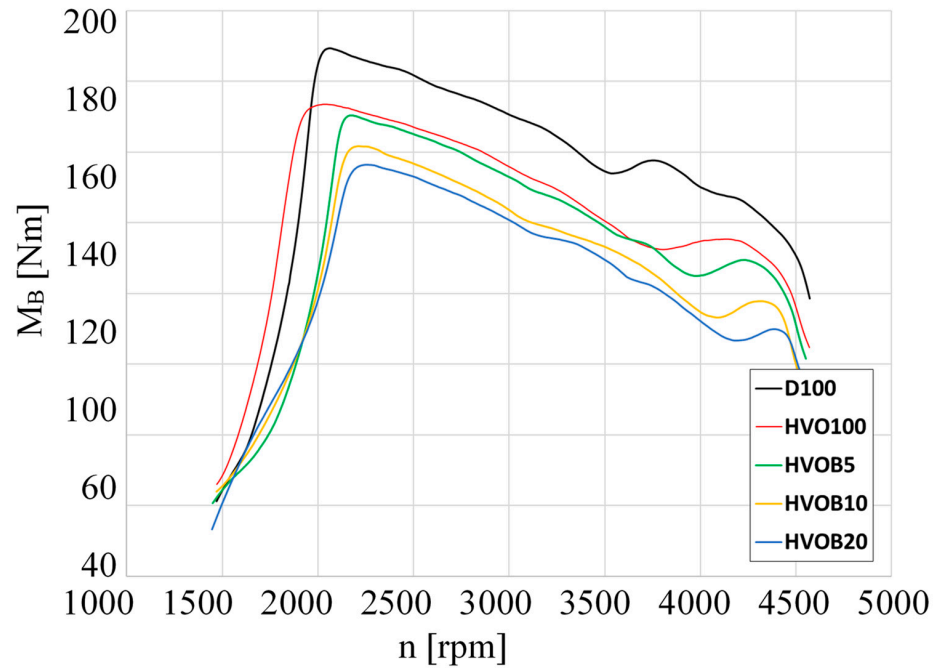


Figure 2. Engine load depending on fuel composition at different engine speeds.

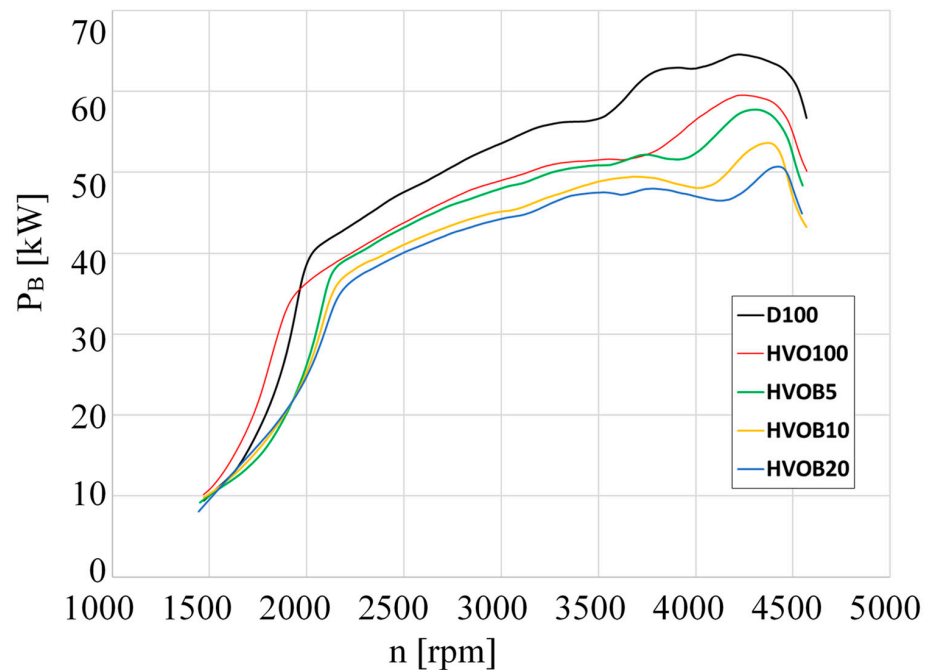


Figure 3. Engine power depending on fuel composition at different engine speeds.

Table 5. The Pearson correlation coefficient values pertaining to various types of fuels.

Engine's Parameter	n [rpm]	P-Norm [kW]	M-Norm [Nm]	b _e [g/kWh]	η _e	Lambda	SOI [CAD BTDC]	m _{air} [mg/cycle]	m _f [mg/cycle]
D100									
n [rpm]	1.000	0.898	0.249	−0.684	0.712	0.126	0.974	−0.519	−0.632
P-norm [kW]	0.898	1.000	0.638	−0.894	0.903	0.313	0.959	−0.112	−0.254
M-norm [Nm]	0.249	0.638	1.000	−0.848	0.819	0.646	0.411	0.677	0.491
b _e [g/kWh]	−0.684	−0.894	−0.848	1.000	−0.984	−0.665	−0.774	−0.243	0.002
η _e	0.712	0.903	0.819	−0.984	1.000	0.669	0.778	0.167	−0.094
lambda	0.126	0.313	0.646	−0.665	0.669	1.000	0.145	0.471	0.109
SOI [CAD BTDC]	0.974	0.959	0.411	−0.774	0.778	0.145	1.000	−0.347	−0.445
m _{air} [mg/cycle]	−0.519	−0.112	0.677	−0.243	0.167	0.471	−0.347	1.000	0.928
m _f [mg/cycle]	−0.632	−0.254	0.491	0.002	−0.094	0.109	−0.445	0.928	1.000
HVO100									
n [rpm]	1.000	0.885	0.121	−0.667	0.668	0.355	0.969	−0.234	−0.334
P-norm [kW]	0.885	1.000	0.555	−0.840	0.809	0.399	0.969	0.212	0.114
M-norm [Nm]	0.121	0.555	1.000	−0.711	0.646	0.436	0.344	0.903	0.802
b _e [g/kWh]	−0.667	−0.840	−0.711	1.000	−0.987	−0.773	−0.757	−0.397	−0.174
η _e	0.668	0.809	0.646	−0.987	1.000	0.786	0.733	0.303	0.068
lambda	0.355	0.399	0.436	−0.773	0.786	1.000	0.358	0.286	−0.023
SOI [CAD BTDC]	0.969	0.969	0.344	−0.757	0.733	0.358	1.000	−0.004	−0.094
m _{air} [mg/cycle]	−0.234	0.212	0.903	−0.397	0.303	0.286	−0.004	1.000	0.951
m _f [mg/cycle]	−0.334	0.114	0.802	−0.174	0.068	−0.023	−0.094	0.951	1.000
HVOB5									
n [rpm]	1.000	0.840	−0.188	−0.448	0.413	−0.405	0.988	−0.709	−0.588
P-norm [kW]	0.840	1.000	0.357	−0.771	0.718	−0.454	0.897	−0.231	−0.084
M-norm [Nm]	−0.188	0.357	1.000	−0.729	0.705	0.076	−0.071	0.808	0.803
b _e [g/kWh]	−0.448	−0.771	−0.729	1.000	−0.990	−0.113	−0.513	−0.220	−0.194
η _e	0.413	0.718	0.705	−0.990	1.000	0.210	0.462	0.204	0.146
lambda	−0.405	−0.454	0.076	−0.113	0.210	1.000	−0.469	0.221	−0.091
SOI [CAD BTDC]	0.988	0.897	−0.071	−0.513	0.462	−0.469	1.000	−0.607	−0.462
m _{air} [mg/cycle]	−0.709	−0.231	0.808	−0.220	0.204	0.221	−0.607	1.000	0.951
m _f [mg/cycle]	−0.588	−0.084	0.803	−0.194	0.146	−0.091	−0.462	0.951	1.000
HVOB10									
n [rpm]	1.000	0.814	−0.161	−0.423	0.367	0.176	0.979	−0.340	−0.373
P-norm [kW]	0.814	1.000	0.421	−0.751	0.683	0.241	0.889	0.235	0.218
M-norm [Nm]	−0.161	0.421	1.000	−0.737	0.722	0.382	−0.031	0.966	0.917
b _e [g/kWh]	−0.423	−0.751	−0.737	1.000	−0.992	−0.729	−0.459	−0.584	−0.425
η _e	0.367	0.683	0.722	−0.992	1.000	0.765	0.388	0.565	0.391
lambda	0.176	0.241	0.382	−0.729	0.765	1.000	0.103	0.333	0.064
SOI [CAD BTDC]	0.979	0.889	−0.031	−0.459	0.388	0.103	1.000	−0.204	−0.204
m _{air} [mg/cycle]	−0.340	0.235	0.966	−0.584	0.565	0.333	−0.204	1.000	0.961
m _f [mg/cycle]	−0.373	0.218	0.917	−0.425	0.391	0.064	−0.204	0.961	1.000
HVOB20									
n [rpm]	1.000	0.850	0.125	−0.560	0.494	0.246	0.985	−0.186	−0.241
P-norm [kW]	0.850	1.000	0.616	−0.861	0.823	0.335	0.917	0.321	0.276
M-norm [Nm]	0.125	0.616	1.000	−0.860	0.884	0.452	0.267	0.915	0.849
b _e [g/kWh]	−0.560	−0.861	−0.860	1.000	−0.982	−0.656	−0.661	−0.667	−0.527
η _e	0.494	0.823	0.884	−0.982	1.000	0.643	0.590	0.666	0.524
lambda	0.246	0.335	0.452	−0.656	0.643	1.000	0.260	0.389	0.091
SOI [CAD BTDC]	0.985	0.917	0.267	−0.661	0.590	0.260	1.000	−0.031	−0.076
m _{air} [mg/cycle]	−0.186	0.321	0.915	−0.667	0.666	0.389	−0.031	1.000	0.951
m _f [mg/cycle]	−0.241	0.276	0.849	−0.527	0.524	0.091	−0.076	0.951	1.000

Figure 4 depicts the fuel mass consumption per cycle (m_f) as a function of fuel composition across various engine speeds. Based on the findings of the conducted research, it is evident that the greatest levels of fuel consumption are observed when employing ordinary diesel fuel, specifically at an engine speed of 1500 rpm. Following the substitution of the fuel with HVO100 and the subsequent introduction of biobutanol in several concentrations ranging from 5% to 20%, a consistent decline in the aforementioned value was observed. Specifically, the reduction percentages were as follows: HVO100—17%, HVOB5—18%, HVOB10—19%, and HVOB20—20%. When the engine speed reaches 4500 rpm when using HVO fuel and its blends with biobutanol, a little alteration in the trend is observed: the mass fraction (m_f) value of HVO100 fuel is approximately 17% lower in comparison to D100. The use of HVOB5, HVOB10, and HVOB20 resulted in a decrease of approximately 2.4% as compared to the use of D100.

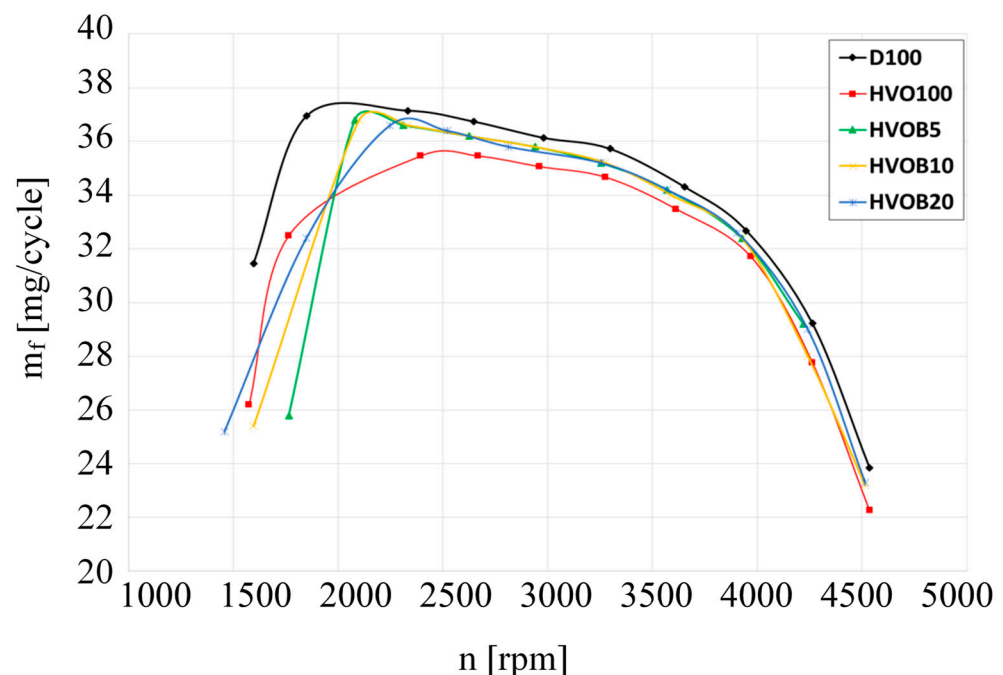


Figure 4. Fuel mass consumption per cycle depending on fuel composition at different engine speeds.

The air mass consumptions for each cycle, denoted as m_{air} , are depicted in Figure 5. The use of D100 fuel resulted in the maximum air mass at a low engine speed of 1500 rpm. After transitioning the fuels to HVO100, there was an observed reduction of around 17% in this value. Additionally, as the concentration of biobutanol in HVO fuel was further raised from 5% to 20%, there was a consistent decrease in this value throughout the different fuel blends. Specifically, the reductions were as follows: HVOB5—18%, HVOB10—19%, and HVOB20—24% when compared to D100. In this particular scenario, the introduction of biobutanol into HVO fuel results in the presence of oxygen alongside biobutanol. Consequently, the resulting m_{air} values exhibit a decrease in comparison to those observed in conventional diesel. When the engine speed reaches 4500 rpm when using HVO fuel and its blends with biobutanol, the observed trend remains consistent, albeit with slightly smaller variations in the drop compared to D100, ranging from 1% to 3.5%.

The air intake system of a compression ignition engine functions with an abundance of air, as depicted in Figure 6. Based on the obtained results, it can be observed that at an engine speed of 1500 rpm, the excess air ratio of HVO100 is decreased by 3% compared to conventional diesel, depending on the engine speed. Nevertheless, the introduction of biobutanol to HVO resulted in an increase in the excess air ratio. The addition of biobutanol at a concentration of 5% (referred to as HVOB5) resulted in a 12% increase, while the

addition of biobutanol at a concentration of 10% (referred to as HVOB10) yielded a value equivalent to that of D100. Nevertheless, when the concentration of biobutanol in HVO fuel was increased to 20%, it was observed that the excess air ratio value was lower compared to that of conventional diesel, namely at 2.2%. The engine speed reached a maximum of 4500 rpm when using HVO100, HVOB10, and HVOB20 fuels. The air surplus values for these fuels were slightly higher, ranging from 0.6% to 1.8%, compared to ordinary diesel. The value of HVOB5 fuel was 1.2% lower compared to D100. The air-to-fuel ratio parameter determines the concentration of unburned hydrocarbons.

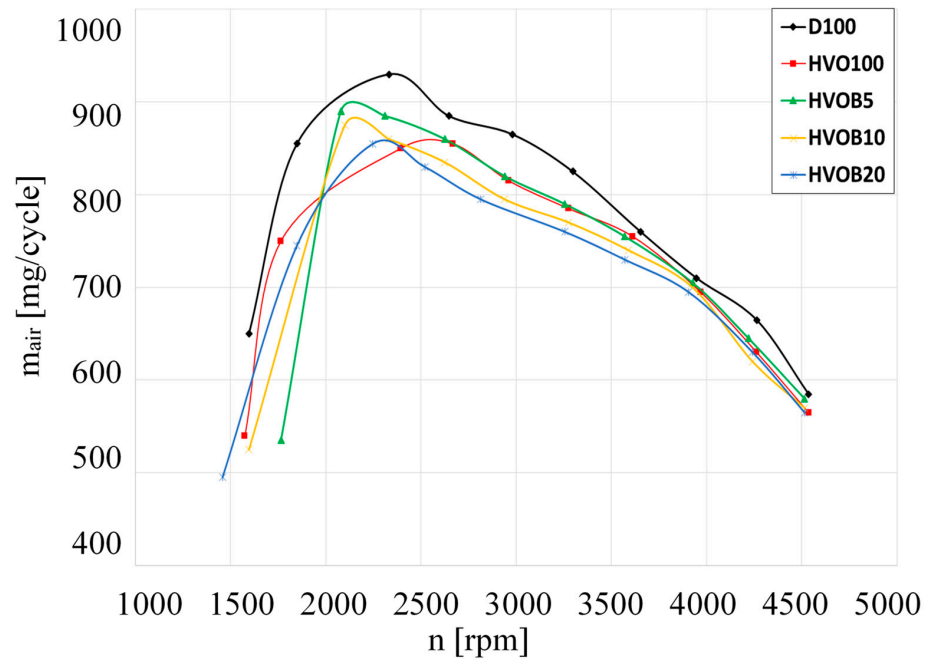


Figure 5. The dependence of air mass consumption per cycle on fuel composition at different engine speeds.

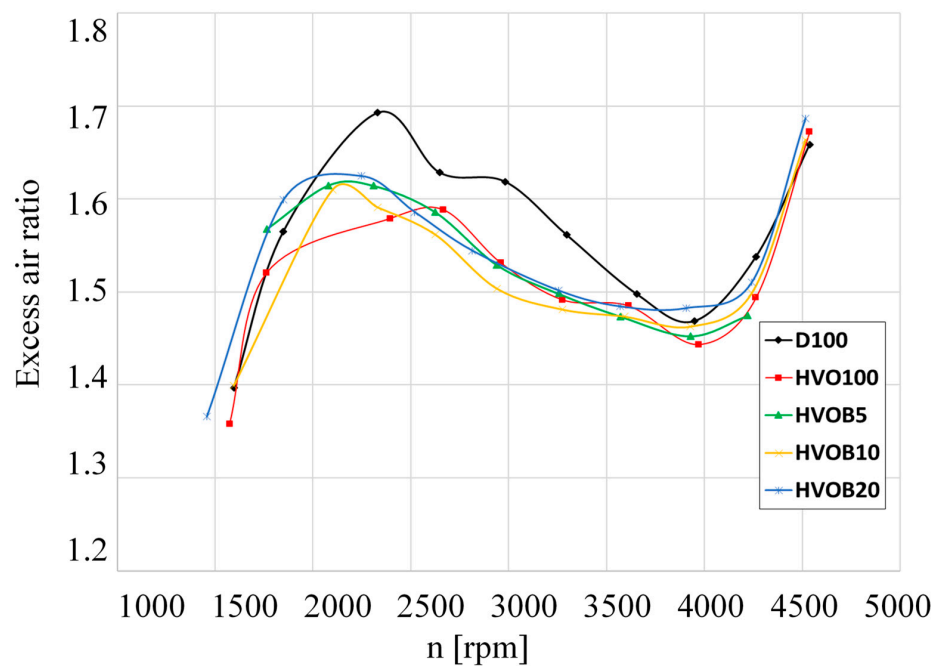


Figure 6. The dependence of excess air ratio on fuel composition at different engine speeds.

The brake-specific fuel mass consumption (BSFC) of the compression ignition engine is depicted in Figure 7. At an engine speed of 1500 rpm, the fuel mass consumption of HVO100, HVOB5, and HVOB10 is observed to be approximately 23% to 24% lower than that of D100. When biobutanol was incorporated into HVO at a concentration of up to 20%, the brake-specific fuel consumption (BSFC) exhibited a 7% increase in comparison to the use of pure diesel fuel (D100). When the engine speed is raised to 4500 rpm, the brake-specific fuel consumption (BSFC) of HVO fuel and blends of HVO and biobutanol (ranging from 5% to 20%) consistently exhibited higher values compared to D100. Specifically, the BSFC values for HVO100, HVOB5, HVOB10, and HVOB20 were found to be 1.7%, 10%, 19%, and 28% higher, respectively, than those of D100. Based on the findings of the fuel analysis (Tables 1 and 2), it can be shown that the lower heating value of HVO100 by mass (MJ/kg), denoted as LHV_m, exhibited a 2.3% increase compared to D100. As the LHV_m value decreases, higher values of BSFC are obtained. The lower heating value (LHV_m) of the HVOB5 fuel mix was observed to be 1% greater compared to D100. Conversely, the LHV_m of HVOB10 was found to be 0.3% lower, while the LHV_m of HVOB20 was 2.8% lower, both in comparison to D100. The significance of brake-specific fuel consumption (BSFC) varies not only due to changes in LHV_m but also due to the engine brake thermal efficiency (Figure 8), which is influenced by the combustion process.

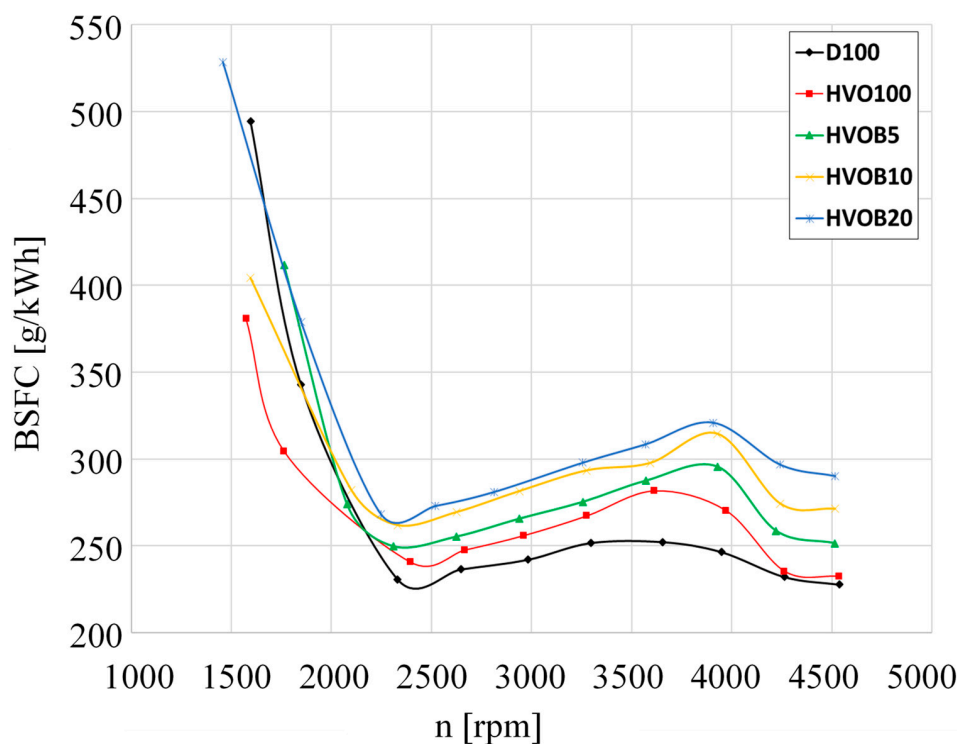


Figure 7. The dependence of BSFC by mass on fuel composition at different engine speeds.

Figure 8 depicts the variation in brake thermal efficiency as a function of engine speed, ranging from 1500 rpm to 4500 rpm. The brake thermal efficiency (BTE) value of HVO100 was approximately 26% higher than that of D100 when operating at 1500 rpm. By elevating the biobutanol concentration in HVO fuel from 5% to 10%, a notable increase in the brake thermal efficiency (BTE) value of around 19% to 22% was observed in comparison to D100. However, when the biobutanol concentration reached 20% in HVO fuel, a decline of approximately 3.5% in BTE value was observed in comparison to D100. Nevertheless, the impact of biobutanol on thermal efficiency diminished as the engine speed increased. The brake thermal efficiency (BTE) of the D100 experienced a drop of around 4.4% at a constant engine speed of 4500 rpm. After increasing the concentration of biobutanol in HVO from 5% to 20%, it was observed that the brake thermal efficiency (BTE) value fell in comparison

to D100. Specifically, the BTE value declined by approximately 10% with HVOB5, 16% with HVOB10, and 20% with HVOB20. The introduction of hydrogenated vegetable oil (HVO) and various combinations of HVO and biobutanol, coupled with an elevation in engine speed, reveals a discernible adverse impact of biobutanol on brake thermal efficiency (BTE).

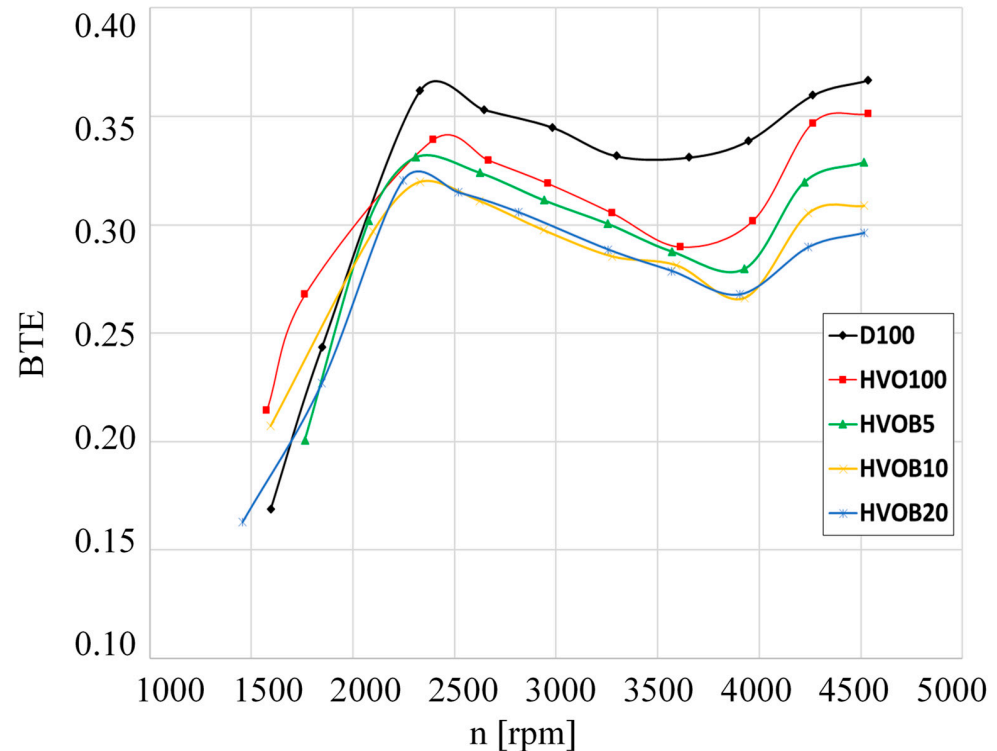


Figure 8. The dependence of brake thermal efficiency on fuel composition at different engine speeds.

The commencement of fuel injection, as shown by the start of injection (SOI) values, exhibited a consistent upward trend in direct correlation with the progressive escalation of engine speed, ranging from 1500 rpm to 4500 rpm. Based on the graphical representation, it is evident that the Start of Injection (SOI) values for various fuels and fuel mixes exhibit disparity when the engine operates at around 1500 revolutions per minute (rpm). In this specific engine mode, the SOI values were observed to vary. The D100 value corresponds to a crank angle degree (CAD) of around 2.6. The parameter known as Before Top Dead Center (BTDC) is denoted by HVO100 and has a value of around 1.3 CAD. Based on the data provided, it can be observed that the BTDC (Before Top Dead Center) timings for HVOB5, HVOB10, and HVOB20 are around 3.5 CAD, 3.6 CAD, and 1.3 CAD, respectively. It is worth noting that the HVOB20 timing exhibits a delay of 1.3 CAD compared to the D100 reference. The State of Interest (SOI) was regulated by the Electronic Control Unit (ECU). Various SOI values were acquired as a result of the distinct physicochemical characteristics of the fuel. At the maximum engine speed of around 4500 revolutions per minute (rpm), the disparities in Start of Injection (SOI) between various fuels and their combinations exhibited reduced magnitudes (Figure 9). The ignition timing for D100 is seen to be 15.0 CAD before top dead center (BTDC), while HVO100 exhibits an ignition timing of 15.6 CAD BTDC. Similarly, HVOB5 demonstrates an ignition timing of 15.8 CAD BTDC, HVOB10 exhibits an ignition timing of 15.4 CAD BTDC, and HVOB20 also displays an ignition timing of 15.4 CAD BTDC, which is 0.4 CAD sooner compared to D100. In summary, the delay values exhibited a modest decrease within a limited range as the engine speed increased up to 4500 rpm when employing HVO and HVO fuel combinations.

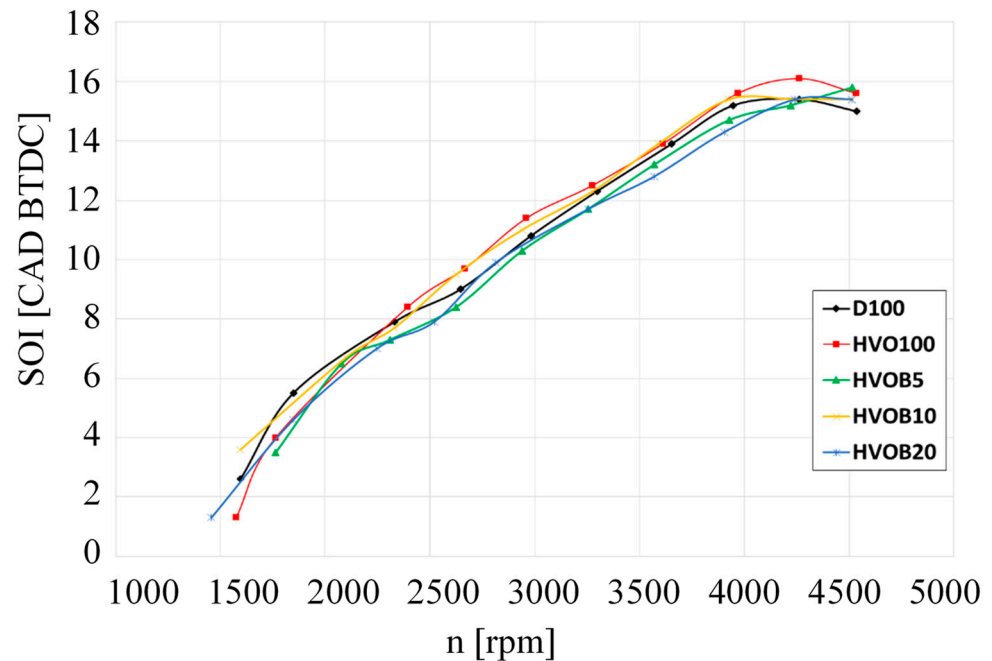


Figure 9. The start of injection depending on the fuel composition at different engine speeds.

4. Discussion

When using various fuel sources, it is crucial to ascertain the parameters of interdependence alterations, which are evident in the correlation between distinct variables. Correlation enables the description of the patterns of co-variation between variables as well as the deliberate justification of the magnitude of relationships between variables. Various types of biofuels and their respective blends were used in the present investigation, alongside regular diesel fuel, which served as a reference for comparative analysis. To expedite the assessment of the impact of fuel type modifications on dependency strength, correlation dependencies were employed. These dependencies are visually depicted in Figures 10–14 and quantitatively summarized in Table 5.

Upon closer inspection of Figure 10, it becomes clear that different fuel types result in the emergence of distinct inter-parameter connection patterns that are analogous to those previously observed. It is essential to recognize the interrelationships between revolutions and power, revolutions and SOI, power and engine speed, power and SOI, efficiency ratio, and fuel consumption, as well as the reciprocal influences of fuel and air masses. While emphasizing a robust connection ranging from 0.999 to 0.800, it is imperative to acknowledge the interrelationships between revolutions and power, revolutions, and SOI. When biofuels are used, whether in their unadulterated form or when combined with other substances, a strong connection may be seen developing between the load, the fuel mass, and the air mass.

While analyzing the correlations across individual biofuels and conducting comparisons between them, it is noted that the variations are less than 10%. This finding suggests that the parameters exhibit independent correlations regardless of the biofuel category. However, it is important to note that the parameters are not similar and exhibit variations based on the specific biofuel being considered.

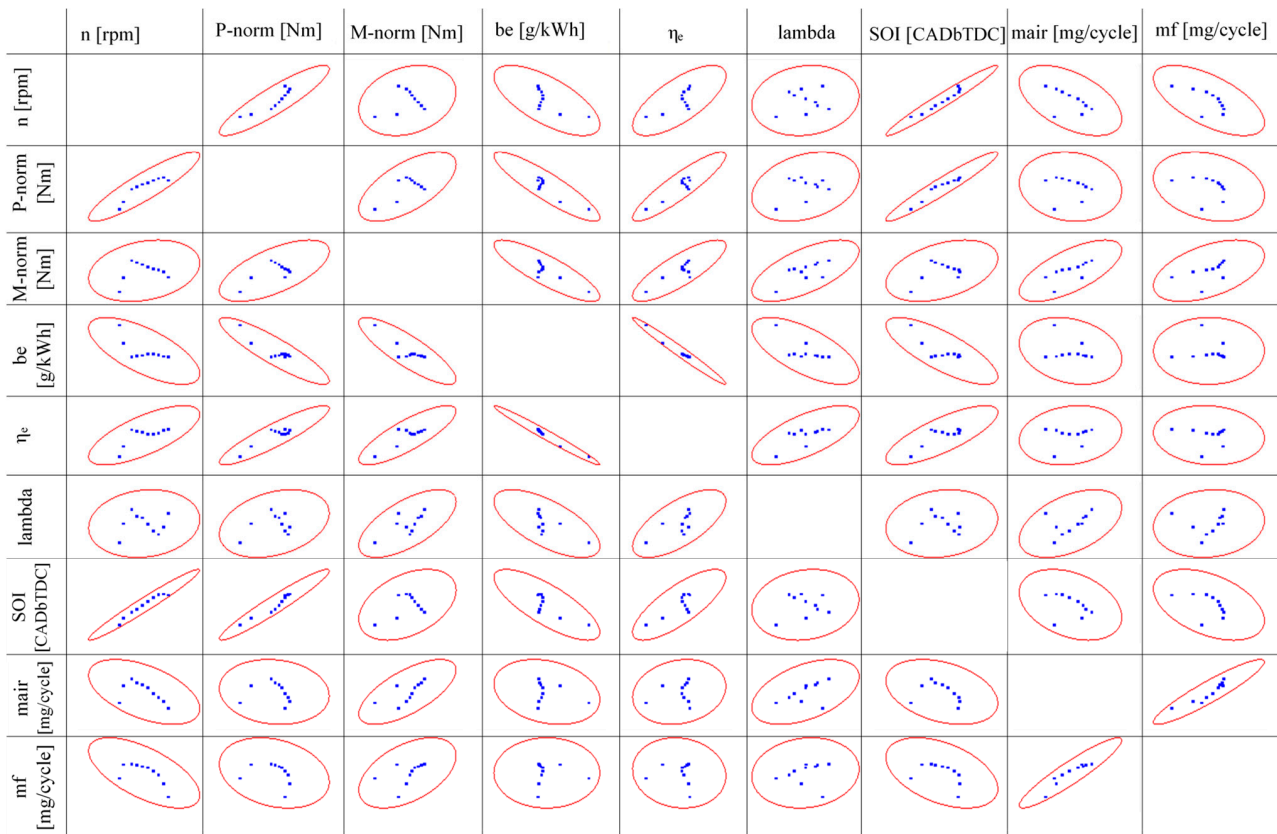


Figure 10. Correlation parameters of engine parameters using different fuels: D100.

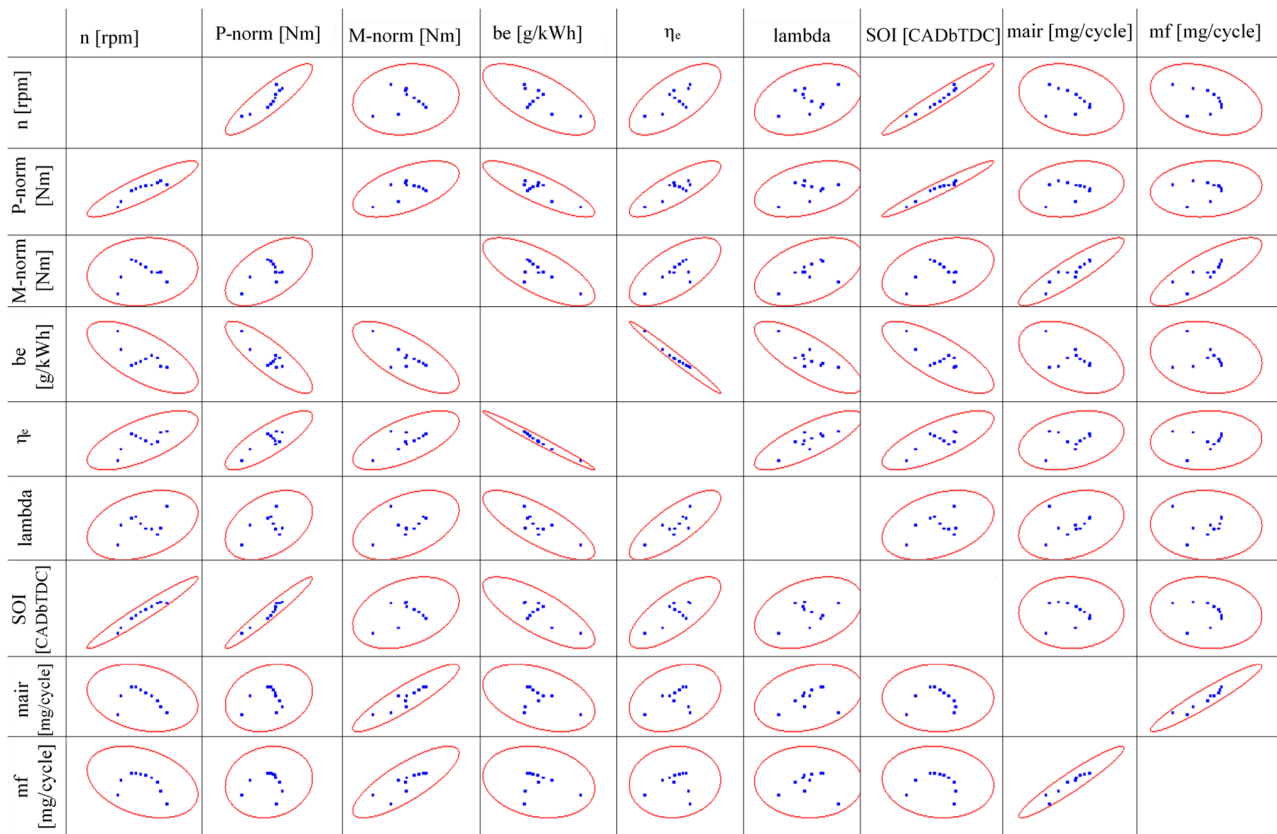


Figure 11. Correlation parameters of engine parameters using different fuels: HVO100.

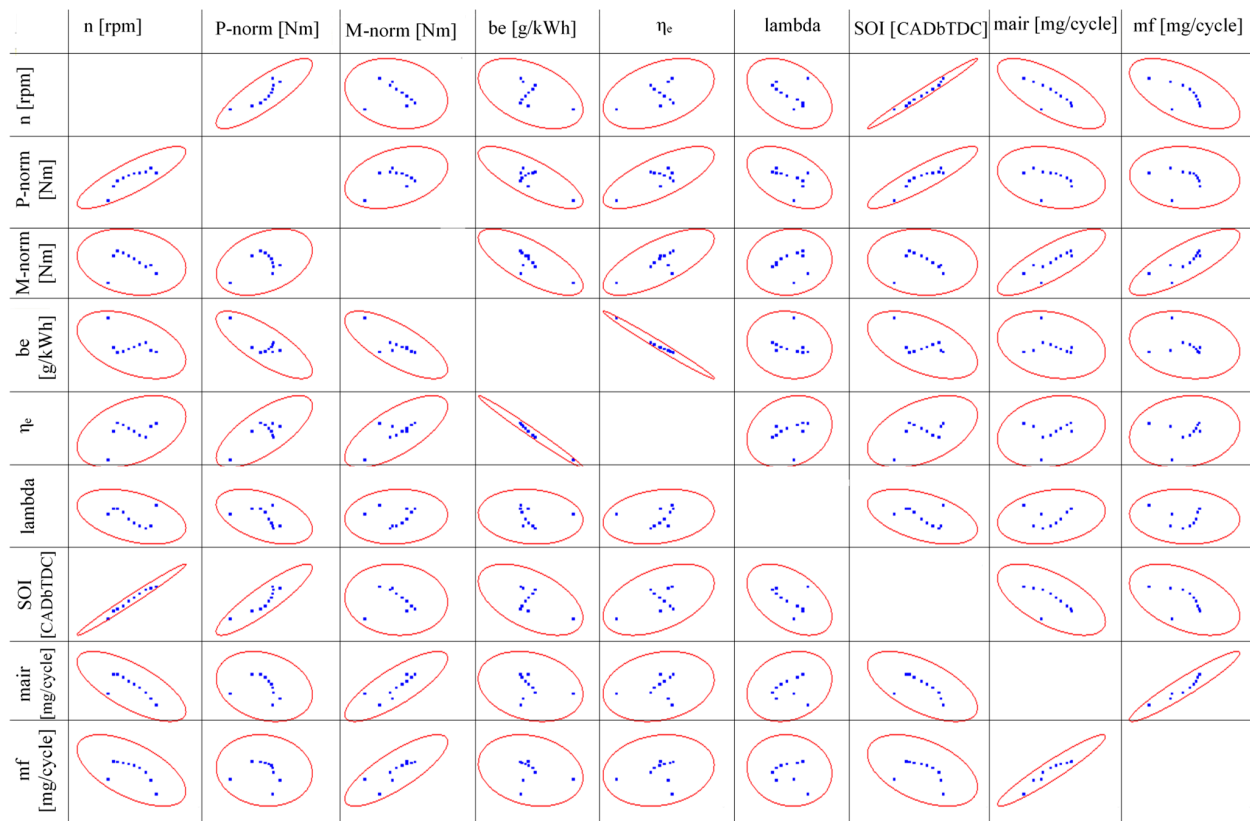


Figure 12. Correlation parameters of engine parameters using different fuels: HVOB5.

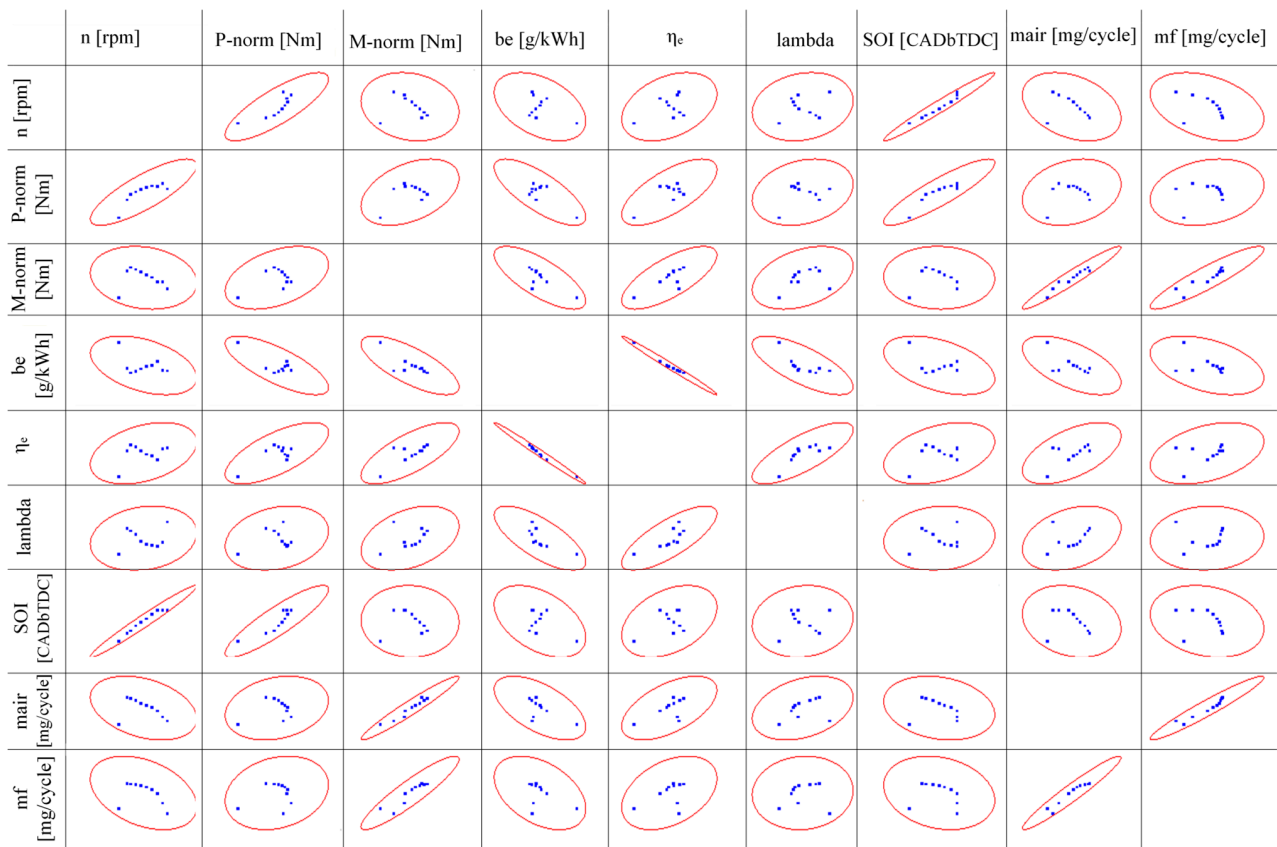


Figure 13. Correlation parameters of engine parameters using different fuels: HVOB10.

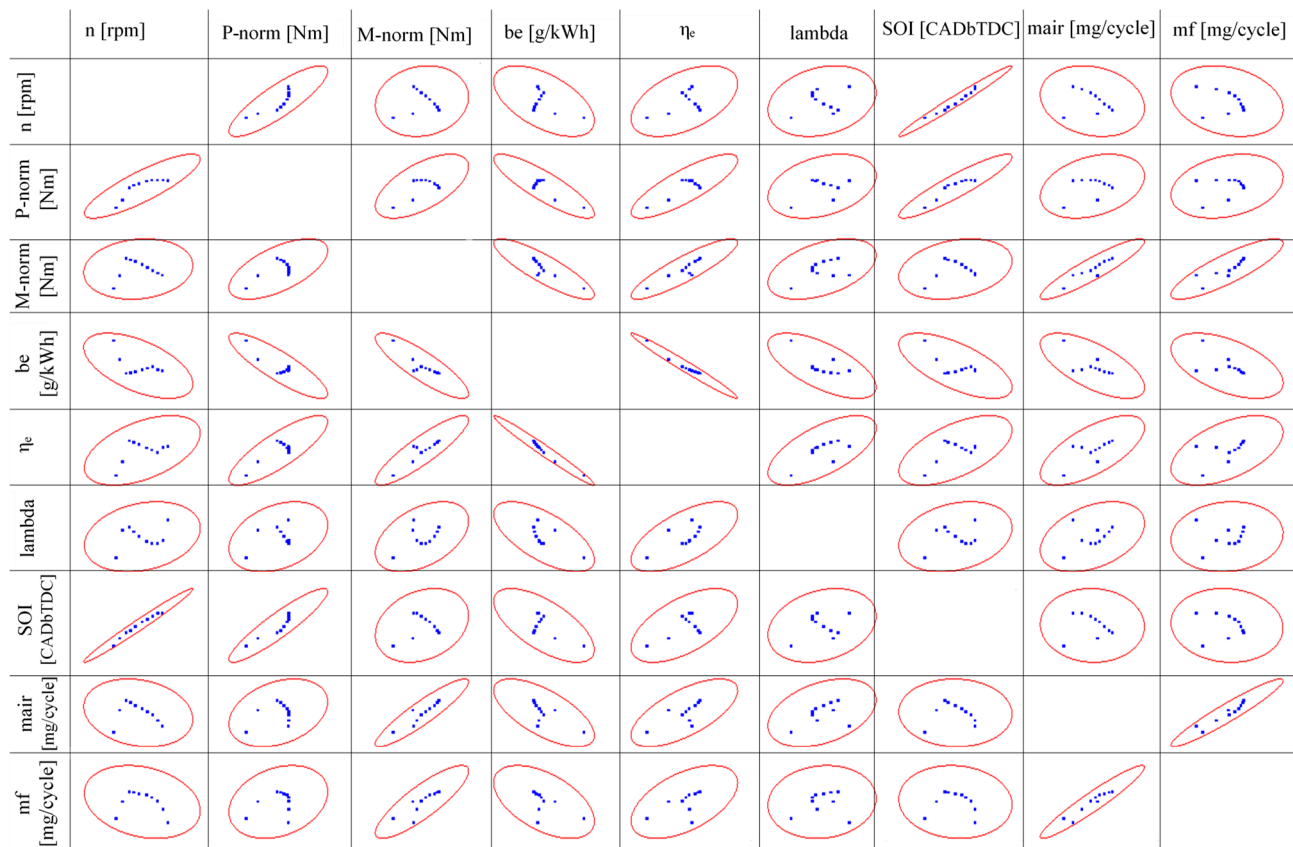


Figure 14. Correlation parameters of engine parameters using different fuels: HVOB20.

5. Conclusions

The analysis carried out allowed for the following conclusions:

- The maximum power output of D100 gasoline is 64.5 kW. However, when using HVO100 fuel, there is an 8% loss in power output. Similarly, HVOB5 fuel results in an 11% decrease, HVOB10 fuel leads to a 17% decrease, and HVOB20 fuel causes a 22% decrease in power output.
- The research conducted revealed that the mass fraction (mf) of HVO100 fuel experiences a reduction of 17% when blended with biobutanol as the engine speed hits 4500 rpm. Additionally, a little alteration in the observed trend is observed at this specific engine speed.
- The use of D100 fuel resulted in the attainment of the highest air mass at an engine speed of 1500 revolutions per minute (rpm). However, the subsequent switch to HVO100 fuel led to a reduction of approximately 17% in the aforementioned air mass. The values of HVOB5, HVOB10, and HVOB20 dropped as the concentration of biobutanol grew from 5% to 20%.
- The brake-specific fuel consumption (BSFC) of HVO fuel and various blends of HVO and biobutanol consistently demonstrates superior performance compared to D100, exhibiting a range of values that consistently surpass D100 by 1.7% to 28%.
- The brake thermal efficiency of the D100 had a decline of 4.4% at an engine speed of 4500 rpm. Furthermore, augmenting the concentration of biobutanol in HVO led to a reduction in the brake thermal efficiency value.
- The Start of Injection (SOI) values exhibit variations across different fuels and mixtures during engine operation at 1500 rpm. The timings for Before Top Dead Center (BTDC) for HVOB5, HVOB10, and HVOB20 exhibit variations of 3.5 CAD, 3.6 CAD, and 1.3 CAD, respectively. Notably, the timing for HVOB20 demonstrates a delay of 1.3 CAD.

Author Contributions: Conceptualization, G.V., J.M. and O.O.; methodology, G.V., J.M., O.O., A.R., A.K. and K.T.; software, A.K., K.T. and A.R.; validation, O.O. and J.M.; formal analysis, J.M., O.O., A.K. and K.T.; investigation, A.R. and G.V.; data curation, J.M., O.O., G.V., A.K., K.T. and A.R.; writing—original draft preparation, G.V., J.M., O.O., A.K. and K.T.; writing—review and editing, G.V., J.M., O.O., A.R. and K.T.; visualization, G.V., J.M., O.O., A.R. and K.T.; supervision, G.V., J.M., O.O., A.R. and K.T. All authors have read and agreed to the published version of the manuscript.

Funding: The research was carried out under financial support obtained from the research subsidy of the Faculty of Engineering Management (WIZ) of Bialystok University of Technology, grant No. WZ/WIZ-INZ/4/2022 (Olga Orynycz). Research was conducted in part during cooperation stays at Vilnius University of Technology (Lithuania 2023). This research was also funded by the Institute of Mechanical Engineering, Warsaw University of Life Sciences.

Data Availability Statement: Data are contained within the article.

Conflicts of Interest: The authors declare no conflict of interest.

References

- Rakov, V. Determination of optimal characteristics of braking energy recovery system in vehicles operating in urban conditions. *Transp. Res. Procedia* **2020**, *50*, 566–573. [CrossRef]
- Krzywonos, M.; Skudlarski, J.; Kupczyk, A.; Wojdalski, J.; Tucki, K. Forecast for transport biofuels in Poland in 2020–2030. *Przem. Chem.* **2015**, *94*, 2218–2222. [CrossRef]
- Robaina, M.; Neves, A. Complete decomposition analysis of CO₂ emissions intensity in the transport sector in Europe. *Res. Transp. Econ.* **2021**, *90*, 101074. [CrossRef]
- Sarkan, B.; Skrucany, T.; Semanova, S.; Madlenak, R.; Kuranc, A.; Sejkorova, M.; Caban, J. Vehicle coast-down method as a tool for calculating total resistance for the purposes of type-approval fuel consumption. *Sci. J. Silesian Univ. Technol. -Ser. Transp.* **2018**, *98*, 161–172.
- CO₂ Emissions from Cars: Facts and Figures (Infographics). Available online: <https://www.europarl.europa.eu/news/en/headlines/society/20190313STO31218/co2-emissions-from-cars-facts-and-figures-infographics> (accessed on 8 October 2023).
- Fact Sheets on the European Union. Energy Policy: General Principles. Available online: <https://www.europarl.europa.eu/factsheets/en/sheet/68/energy-policy-general-principles> (accessed on 8 October 2023).
- Presno, M.J.; Landajo, M.; González, P.F. GHG emissions in the EU-28. A multilevel club convergence study of the Emission Trading System and Effort Sharing Decision mechanisms. *Sustain. Prod. Consum.* **2021**, *27*, 998–1009. [CrossRef]
- Jäger-Waldau, A.; Kougias, I.; Taylor, N.; Thiel, C. How photovoltaics can contribute to GHG emission reductions of 55% in the EU by 2030. *Renew. Sustain. Energy Rev.* **2020**, *126*, 109836. [CrossRef]
- Tucki, K.; Krzywonos, M.; Orynycz, O.; Kupczyk, A.; Bączyk, A.; Wielewska, I. Analysis of the Possibility of Fulfilling the Paris Agreement by the Visegrad Group Countries. *Sustainability* **2021**, *13*, 8826. [CrossRef]
- Clean Energy for All Europeans Package. Available online: https://energy.ec.europa.eu/topics/energy-strategy/clean-energy-all-europeans-package_en (accessed on 8 October 2023).
- Neves, S.A.; Marques, A.C.; Patrício, M. Determinants of CO₂ emissions in European Union countries: Does environmental regulation reduce environmental pollution? *Econ. Anal. Policy* **2020**, *68*, 114–125. [CrossRef]
- Hooftman, N.; Messagie, M.; Van Mierlo, J.; Coosemans, T. A review of the European passenger car regulations—Real driving emissions vs local air quality. *Renew. Sustain. Energy Rev.* **2018**, *86*, 1–21. [CrossRef]
- Cha, J.; Lee, J.; Chon, M.S. Evaluation of real driving emissions for Euro 6 light-duty diesel vehicles equipped with LNT and SCR on domestic sales in Korea. *Atmos. Environ.* **2019**, *196*, 133–142. [CrossRef]
- Tucki, K.; Orynycz, O.; Wasiak, A.; Świć, A.; Mruk, R.; Botwińska, K. Estimation of Carbon Dioxide Emissions from a Diesel Engine Powered by Lignocellulose Derived Fuel for Better Management of Fuel Production. *Energies* **2020**, *13*, 561. [CrossRef]
- Chen, L.; Wang, Z.; Liu, S.; Qu, L. Using a chassis dynamometer to determine the influencing factors for the emissions of Euro VI vehicles. *Transp. Res. Part D Transp. Environ.* **2018**, *65*, 564–573. [CrossRef]
- Mera, Z.; Fonseca, N.; López, J.M.; Casanova, J. Analysis of the high instantaneous NO_x emissions from Euro 6 diesel passenger cars under real driving conditions. *Appl. Energy* **2019**, *242*, 1074–1089. [CrossRef]
- Triantafyllopoulos, G.; Dimaratos, A.; Ntziachristos, L.; Bernard, Y.; Dornoff, J.; Samaras, Z. A study on the CO₂ and NO_x emissions performance of Euro 6 diesel vehicles under various chassis dynamometer and on-road conditions including latest regulatory provisions. *Sci. Total Environ.* **2019**, *666*, 337–346. [CrossRef] [PubMed]
- May, J.; Favre, C.; Bosteels, D.; Andersson, J.; Clarke, D.; Heaney, M. On-Road Testing and PEMS Data Analysis for Two Euro 6 Diesel Vehicles. Available online: <http://www.aecc.eu/wp-content/uploads/2016/08/140918-AECC-paper-on-RDE-TAP-Conference-Graz.pdf> (accessed on 8 October 2023).
- Olabi, A.G.; Maizak, D.; Wilberforce, T. Review of the regulations and techniques to eliminate toxic emissions from diesel engine cars. *Sci. Total Environ.* **2020**, *748*, 141249. [CrossRef] [PubMed]

20. Note on the Application of Regulation (EU) 2017/1151 as Amended by Regulation (EU) 2018/1832. Available online: https://circabc.europa.eu/sd/a/a0a73d43-321f-4f01-ae3f-88ef2342f7e0/Final%20joint%20Note%20to%20TCMV%20on%20RDE4-WLTP2_April_2019%20nw.pdf (accessed on 8 October 2023).
21. EU. Emission Standards. Available online: <https://dieselnet.com/standards/eu/ld.php> (accessed on 8 October 2023).
22. Average CO₂ Emissions from New Cars and New Vans Increased again in 2019. Available online: <https://www.eea.europa.eu/highlights/average-co2-emissions-from-new-cars-vans-2019> (accessed on 8 October 2023).
23. Dimaratos, A.; Tsokolis, D.; Fontaras, G.; Tsiakmakis, S.; Ciuffo, B.; Samaras, Z. Comparative Evaluation of the Effect of Various Technologies on Light-duty Vehicle CO₂ Emissions over NEDC and WLTP. *Transp. Res. Procedia* **2016**, *14*, 3169–3178. [[CrossRef](#)]
24. Tucki, K. A Computer Tool for Modelling CO₂ Emissions in Driving Tests for Vehicles with Diesel Engines. *Energies* **2021**, *14*, 266. [[CrossRef](#)]
25. Ko, J.; Jin, D.; Jang, W.; Myung, C.L.; Kwon, S.; Park, S. Comparative investigation of NO_x emission characteristics from a Euro 6-compliant diesel passenger car over the NEDC and WLTC at various ambient temperatures. *Appl. Energy* **2017**, *187*, 652–662. [[CrossRef](#)]
26. Tucki, K. A Computer Tool for Modelling CO₂ Emissions in Driving Cycles for Spark Ignition Engines Powered by Biofuels. *Energies* **2021**, *14*, 1400. [[CrossRef](#)]
27. Blanco-Rodriguez, D.; Vagnoni, G.; Holderbaum, B. EU6 C-Segment Diesel vehicles, a challenging segment to meet RDE and WLTP requirements. *IFAC-Pap.* **2016**, *49*, 649–656. [[CrossRef](#)]
28. Wang, Y.; Ge, Y.; Wang, J.; Wang, X.; Yin, H.; Hao, L.; Tan, J. Impact of altitude on the real driving emission (RDE) results calculated in accordance to moving averaging window (MAW) method. *Fuel* **2020**, *277*, 117929. [[CrossRef](#)]
29. Viesi, D.; Crema, L.; Testi, M. The Italian hydrogen mobility scenario implementing the European directive on alternative fuels infrastructure (DAFI 2014/94/EU). *Int. J. Hydrog. Energy* **2017**, *42*, 27354–27373. [[CrossRef](#)]
30. Ananthi, V.; Raja, R.; Carvalho, I.S.; Brindhadevi, K.; Pugazhendhi, A.; Arun, A. A realistic scenario on microalgae based biodiesel production: Third generation biofuel. *Fuel* **2021**, *284*, 118965. [[CrossRef](#)]
31. Alves-Fortunato, M.; Ayoub, E.; Bacha, K.; Mouret, A.; Dalmazzone, C. Fatty Acids Methyl Esters (FAME) autoxidation: New insights on insoluble deposit formation process in biofuels. *Fuel* **2020**, *268*, 117074. [[CrossRef](#)]
32. Puricelli, S.; Cardellini, G.; Casadei, S.; Faedo, D.; Van den Oever, A.E.M.; Grosso, M. A review on biofuels for light-duty vehicles in Europe. *Renew. Sustain. Energy Rev.* **2020**, *137*, 110398. [[CrossRef](#)]
33. Supporting Policy with Scientific Evidence. Biofuel. Available online: https://knowledge4policy.ec.europa.eu/glossary-item/biofuel_en (accessed on 8 October 2023).
34. Cadillo-Benalcazar, J.J.; Bukkens, S.G.F.; Ripa, M.; Giampietro, M. Why does the European Union produce biofuels? Examining consistency and plausibility in prevailing narratives with quantitative storytelling. *Energy Res. Soc. Sci.* **2021**, *71*, 101810. [[CrossRef](#)]
35. Dafnomilis, I.; Hoefnagels, R.; Pratama, Y.W.; Schott, D.L.; Lodewijks, G.; Junginger, M. Review of solid and liquid biofuel demand and supply in Northwest Europe towards 2030—A comparison of national and regional projections. *Renew. Sustain. Energy Rev.* **2017**, *78*, 31–45. [[CrossRef](#)]
36. Stattman, S.L.; Gupta, A.; Partzsch, L.; Oosterveer, P. Toward Sustainable Biofuels in the European Union? Lessons from a Decade of Hybrid Biofuel Governance. *Sustainability* **2018**, *10*, 4111. [[CrossRef](#)]
37. Bemani, A.; Xiong, Q.; Baghban, A.; Habibzadeh, S.; Mohammadi, A.H.; Doranehgard, M.H. Modeling of cetane number of biodiesel from fatty acid methyl ester (FAME) information using GA-, PSO-, and HGAPSO- LSSVM models. *Renew. Energy* **2020**, *150*, 924–934. [[CrossRef](#)]
38. Verevkin, S.P.; Pimerzin, A.A.; Glotov, A.P.; Vutolkina, A.V. Biofuels energetics: Reconciliation of calorific values of fatty acids methyl esters with help of complementary measurements and structure–property relationships. *Fuel* **2022**, *329*, 125460. [[CrossRef](#)]
39. Ngige, G.A.; Ovuoraye, P.E.; Igwegbe, C.A.; Fetahi, E.; Okeke, J.A.; Yakubu, A.D.; Onyechi, P.C. RSM optimization and yield prediction for biodiesel produced from alkali-catalytic transesterification of pawpaw seed extract: Thermodynamics, kinetics, and Multiple Linear Regression analysis. *Digit. Chem. Eng.* **2023**, *6*, 100066. [[CrossRef](#)]
40. Bolonio, D.; García-Martínez, M.J.; Ortega, M.F.; Lapuerta, M.; Rodríguez-Fernández, J.; Canoira, L. Fatty acid ethyl esters (FAEEs) obtained from grapeseed oil: A fully renewable biofuel. *Renew. Energy* **2019**, *132*, 278–283. [[CrossRef](#)]
41. Suarez-Bertoa, R.; Kousoulidou, M.; Clairotte, M.; Giechaskiel, B.; Nuottimäki, J.; Sarjoavaara, T.; Lonza, L. Impact of HVO blends on modern diesel passenger cars emissions during real world operation. *Fuel* **2019**, *235*, 1427–1435. [[CrossRef](#)]
42. McCaffery, C.; Zhu, H.; Ahmed, C.M.S.; Canchola, A.; Chen, J.Y.; Li, C.; Johnson, K.C.; Durbin, T.D.; Lin, Y.H.; Karavalakis, G. Effects of hydrogenated vegetable oil (HVO) and HVO/biodiesel blends on the physicochemical and toxicological properties of emissions from an off-road heavy-duty diesel engine. *Fuel* **2022**, *323*, 124283. [[CrossRef](#)]
43. Dimitriadis, A.; Natsios, I.; Dimaratos, A.; Katsaounis, D.; Samaras, Z. Hydrotreated Vegetable Oil (HVO) and Effects on Emissions of a Passenger Car Diesel Engine. *Front. Mech. Eng.* **2018**, *4*, 7. [[CrossRef](#)]
44. Rajak, U.; Nashine, P.; Verma, T.N.; Pugazhendhi, A. Performance and emission analysis of a diesel engine using hydrogen enriched n-butanol, diethyl ester and Spirulina microalgae biodiesel. *Fuel* **2020**, *271*, 117645. [[CrossRef](#)]
45. Maroušek, J.; Strunecký, O.; Bartoš, V.; Vochozka, M. Revisiting competitiveness of hydrogen and algae biodiesel. *Fuel* **2022**, *328*, 125317. [[CrossRef](#)]

46. Liao, Y.; Tozluoğlu, C.; Sprei, F.; Yeh, S.; Dhamal, S. Impacts of charging behavior on BEV charging infrastructure needs and energy use. *Transp. Res. Part D Transp. Environ.* **2023**, *116*, 103645. [CrossRef]
47. Zhou, W.; Cleaver, C.J.; Dunant, C.F.; Allwood, J.M.; Lin, J. Cost, range anxiety and future electricity supply: A review of how today's technology trends may influence the future uptake of BEVs. *Renew. Sustain. Energy Rev.* **2023**, *173*, 113074. [CrossRef]
48. Suhel, A.; Abdul Rahim, N.; Abdul Rahman, M.R.; Bin Ahmad, K.A. Engine's Behaviour on Magnetite Nanoparticles as Additive and Hydrogen Addition of Chicken Fat Methyl Ester Fuelled DICI Engine: A Dual Fuel Approach. *Int. J. Hydrogen Energy* **2021**, *46*, 14824–14843. [CrossRef]
49. Syed, A.; Quadri, S.A.P.; Rao, G.A.P.; Mohd, W. Experimental investigations on DI (direct injection) diesel engine operated on dual fuel mode with hydrogen and mahua oil methyl ester (MOME) as injected fuels and effects of injection opening pressure. *Appl. Therm. Eng.* **2017**, *114*, 118–129. [CrossRef]
50. Karagöz, Y. Analysis of the impact of gasoline, biogas and biogas + hydrogen fuels on emissions and vehicle performance in the WLTC and NEDC. *Int. J. Hydrogen Energy* **2019**, *44*, 31621–31632. [CrossRef]
51. Deng, B.; Chen, Z.; Sun, C.; Zhang, S.; Yu, W.; Huang, M.; Hou, K.; Ran, J.; Zhou, L.; Chen, C.; et al. Key design and layout factors influencing performance of three-way catalytic converters: Experimental and semidecoupled numerical study under real-life driving conditions. *J. Clean. Prod.* **2023**, *425*, 138993. [CrossRef]
52. Rumbo Morales, J.Y.; Ortiz-Torres, G.; García, R.O.D.; Cantero, C.A.T.; Rodriguez, M.C.; Sarmiento-Bustos, E.; Ocegüera-Contreras, E.; Hernández, A.A.F.; Cerda, J.C.R.; Molina, Y.A.; et al. Review of the Pressure Swing Adsorption Process for the Production of Biofuels and Medical Oxygen: Separation and Purification Technology. *Adsorpt. Sci. Technol.* **2022**, *2022*, 3030519. [CrossRef]
53. Tucki, K.; Orynych, O.; Wasiak, A.; Świć, A.; Wichłacz, J. The Impact of Fuel Type on the Output Parameters of a New Biofuel Burner. *Energies* **2019**, *12*, 1383. [CrossRef]
54. Kosowski, K.; Tucki, K.; Kosowski, A. Application of Artificial Neural Networks in Investigations of Steam Turbine Cascades. *J. Turbomach. -Trans. ASME* **2010**, *132*, 014501–014505. [CrossRef]
55. Valeika, G.; Matijošius, J.; Orynych, O.; Rimkus, A.; Świć, A.; Tucki, K. Smoke Formation during Combustion of Biofuel Blends in the Internal Combustion Compression Ignition Engine. *Energies* **2023**, *16*, 3682. [CrossRef]
56. Shepel, O.; Matijošius, J.; Rimkus, A.; Orynych, O.; Tucki, K.; Świć, A. Combustion, Ecological, and Energetic Indicators for Mixtures of Hydrotreated Vegetable Oil (HVO) with Duck Fat Applied as Fuel in a Compression Ignition Engine. *Energies* **2022**, *15*, 7892. [CrossRef]
57. Rudbāhs, R.; Smigins, R. Experimental research on biodiesel compatibility with fuel system elastomers. In Proceedings of the 13th International Scientific Conference Engineering for Rural Development, Jelgava, Latvia, 29–30 May 2014; Volume 13, pp. 278–282.
58. Duan, X.; Feng, L.; Liu, H.; Jiang, P.; Chen, C.; Sun, Z. Experimental investigation on exhaust emissions of a heavy-duty vehicle powered by a methanol-fuelled spark ignition engine under world Harmonized Transient Cycle and actual on-road driving conditions. *Energy* **2023**, *282*, 128869. [CrossRef]
59. Sarkan, B.; Stopka, O.; Gnap, J.; Caban, J. Investigation of Exhaust Emissions of Vehicles with the Spark Ignition Engine within Emission Control. In Proceedings of the 10th International Scientific Conference on Transportation Science and Technology (TRANSBALTICA), Vilnius, Lithuania, 4–5 May 2017; Volume 187, pp. 775–782. [CrossRef]
60. Martínez García, M.; Rumbo Morales, J.Y.; Torres, G.O.; Rodríguez Paredes, S.A.; Vázquez Reyes, S.; Sorcia Vázquez, F.d.J.; Pérez Vidal, A.F.; Valdez Martínez, J.S.; Pérez Zúñiga, R.; Rentería Vargas, E.M. Simulation and State Feedback Control of a Pressure Swing Adsorption Process to Produce Hydrogen. *Mathematics* **2022**, *10*, 1762. [CrossRef]
61. López Núñez, A.R.; Rumbo Morales, J.Y.; Salas Villalobos, A.U.; De La Cruz-Soto, J.; Ortiz Torres, G.; Rodríguez Cerda, J.C.; Calixto-Rodríguez, M.; Brizuela Mendoza, J.A.; Aguilar Molina, Y.; Zatarain Durán, O.A.; et al. Optimization and Recovery of a Pressure Swing Adsorption Process for the Purification and Production of Bioethanol. *Fermentation* **2022**, *8*, 293. [CrossRef]
62. Abed, K.A.; El Morsi, A.K.; Sayed, M.M.; El Shaib, A.A.; Gad, M.S. Effect of waste cooking-oil biodiesel on performance and exhaust emissions of a diesel engine. *Egypt. J. Pet.* **2018**, *27*, 985–989. [CrossRef]
63. Kanthasamy, P.; Selvan, V.A.M.; Shanmugam, P. Investigation on the performance, emissions and combustion characteristics of CRDI engine fuelled with tallow methyl ester biodiesel blends with exhaust gas recirculation. *J. Therm. Anal. Calorim.* **2020**, *141*, 2325–2333. [CrossRef]
64. Emiroglu, A.O.; Keskin, A.; Sen, M. Experimental investigation of the effects of turkey rendering fat biodiesel on combustion, performance and exhaust emissions of a diesel engine. *Fuel* **2018**, *216*, 266–273. [CrossRef]
65. Specifications for Skoda Octavia 1.9 TDI Generation 1Z. Available online: <https://www.car.info/en-se/skoda/octavia/1z-19-tdi-dct6-24107173/specs> (accessed on 8 October 2023).
66. Emission, Function and Performance Dynamometers. Available online: <https://www.maha.ru/upload/iblock/a8e/a8e11397fb2b2f09876572eb316514b5.pdf> (accessed on 8 October 2023).
67. OBDI/OBDII Diagnostic Interfaces. Available online: https://smartmoto.pl/pol_m_Diagnostyka_Interfejsy-diaagnostyczne_Interfejsy-OBDI-OBDII-1561535.html (accessed on 8 October 2023).
68. ECU Explained. Available online: <https://www.ecutesting.com/categories/ecu-explained/> (accessed on 8 October 2023).
69. ROSS-TECH VCDS. Available online: <https://www.ross-tech.com/vcbs/tour/logging.php> (accessed on 8 October 2023).
70. Wang, T.; Lin, B. Fuel consumption in road transport: A comparative study of China and OECD countries. *J. Clean. Prod.* **2019**, *206*, 156–170. [CrossRef]

71. Kordylewski, W. *Combustion and Fuels*, 5th ed.; Oficyna Wydawnicza Politechniki Wrocławskiej: Wrocław, Poland, 2008; pp. 10–470. ISBN 978-83-7493-378-0.
72. Baczewski, K.; Kałdoński, T. *Fuels For Compression-Ignition Engines*, 2nd ed.; Wydawnictwa Komunikacji i Łączności: Warszawa, Poland, 2017; pp. 50–210.

Disclaimer/Publisher’s Note: The statements, opinions and data contained in all publications are solely those of the individual author(s) and contributor(s) and not of MDPI and/or the editor(s). MDPI and/or the editor(s) disclaim responsibility for any injury to people or property resulting from any ideas, methods, instructions or products referred to in the content.